

A profile tracking system for investigating the behaviour of discharges in moving environments

H. J. Wang, M. J. Davidson

Abstract A profile tracking system (PTS) is developed to make measurements at previously inaccessible dimensionless distances from a discharge in a moving environment. With this system the measuring components remain stationary as the source is towed away from them. Image processing techniques are then employed to track concentration profiles through a sequence of images, which are a constant distance from the flow source. Data obtained from the PTS are shown to be both reliable and accurate. The benefits and limitations of the PTS when compared with normally configured laser-induced fluorescence systems are discussed. PTS is employed to gather data at dimensionless distances that are an order of magnitude greater than those previously obtained for the co-flowing jet problem.

List of symbols

b	spread of the jet
c	local mean tracer concentration
C	centreline mean tracer concentration
C_0	initial tracer concentration
C_r	jet centreline dilution
H_{SCL}	horizontal scaling factor
L_E	effective image length
L_I	image length
M_{e0}	initial excess momentum of the flow per unit density
N_p	profiles per image length
O_I	initial image offset
O_F	final image offset
t_D	sampling time per source location
U_a	ambient fluid velocity
U_{ar}	ambient to initial discharge velocity ratio
u_e	magnitude of the local mean jet excess velocity
U_e	magnitude of the centreline mean jet excess velocity

x	Cartesian coordinate in the same direction as the ambient velocity and the distance from the jet virtual source
Δt	profile sampling rate
λ	difference in the width of the velocity and tracer concentration distributions

1 Introduction

The behaviour of discharges into still and moving environments has been investigated experimentally for many years, but despite this long history there are still regions of discharge behaviour where our understanding of the flow has not been confirmed experimentally. This confirmation has not been obtained because of limitations in experimental facilities and instrumentation. In recent years, relatively new optical techniques, such as laser-induced fluorescence (LIF) and particle image velocimetry (PIV), have provided the basis for very detailed studies into the behaviour of relatively simple discharge configurations. These studies have provided considerable insight into these flows and an excellent example of this is the work of Papantaniou and List (1989). They employed LIF to conduct detailed investigations into the behaviour of jets and plumes in a still ambient fluid.

The LIF technique has enabled investigators to obtain a more detailed understanding of mixing processes, where the mean behaviour of the flow is reasonably well understood. However, with some modification it can also provide the basis for dealing with flows where previously it was not possible to obtain high-quality experimental data. An example of such a flow is the strongly advected co-flowing jet. This type of jet is created when a non-buoyant fluid is released with a velocity (U_0) into an ambient fluid that is non-turbulent, moving in the same direction and has a velocity (U_a). A schematic diagram of such a flow is shown in Fig. 1, where u_e is the jet velocity in excess of the ambient velocity.

With this discharge configuration, there are two distinct forms of self-similar behaviour. Near the source where the centreline excess velocity (U_e) of the jet is much greater than the ambient velocity, the flow behaves like a jet in a still ambient fluid. This we refer to as a weakly advected jet. With increasing distance from the source, the excess velocity decays and eventually this velocity becomes much smaller than the ambient velocity. The flow behaviour in this region is distinctly different from the weakly advected flow, and we refer to it as a strongly advected jet.

Received: 30 June 1999/Accepted: 21 March 2001

H. J. Wang, M. J. Davidson (✉)
Department of Civil Engineering, Hong Kong University of
Science and Technology, Hong Kong

Present address: M. J. Davidson
Department of Civil Engineering
University of Canterbury, Private Bag 4800
Christchurch, New Zealand
e-mail: m.davidson@civil.canterbury.ac.nz

The authors acknowledge the financial support of the Research Grants Council of Hong Kong.

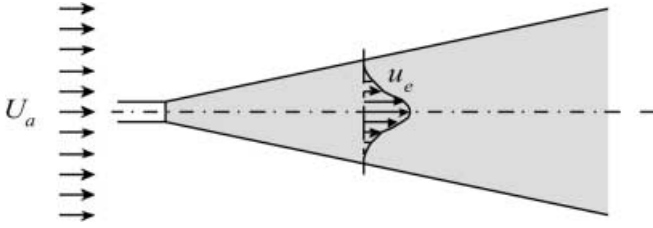


Fig. 1. A schematic diagram of a jet in a co-flowing ambient fluid

Investigation by Smith and Hughes (1977), Antonia and Bilger (1973) and Biringen (1986), for example, have provided experimental information about the behaviour of co-flowing jets. However, it was Patel's (1971) investigation into two-dimensional jets in a co-flowing ambient fluid, which formed the basis for our current understanding of the co-flowing jet problem. Antonia and Bilger (1974) and Knudsen (1988) extended Patel's approach to axisymmetric co-flowing jets. Applying the equations of motion, along with an appropriate spread assumption, reveals that the flow behaviour in the weakly advected region of an axisymmetric co-flowing jet is characterized by:

$$b \propto x^1$$

$$C_r \propto x^1$$

$$U_e \propto x^{-1}$$

where x is the distance from the flow source, b is the jet velocity radius at which $u_e/U_e = e^{-1}$ and C_r is the mean centreline dilution of the jet, that is, the initial tracer concentration (C_0) divided by the local mean centreline tracer concentration (C).

In the strongly advected co-flowing jet region, the behaviour is characterized by:

$$b \propto x^{1/3}$$

$$C_r \propto x^{2/3}$$

$$U_e \propto x^{-2/3}$$

In addition, dimensional analysis indicates that the transition between the weakly and strongly advected flows occurs when the distance from the source (x) is of the order of $M_{e0}^{1/2}/U_a$, where M_{e0} is the initial excess momentum of the flow per unit density.

An important feature of this flow noted by Davidson and Pun (1998) is the length of the transition, which occurs over an order of magnitude of dimensionless distance ($x/(M_{e0}^{1/2}/U_a)$). They indicate the transition begins when this dimensionless distance is of order 1 and nears completion when it is of order 100. It is important to note that existing data sets, including the more recent hot wire measurements of Nickels and Perry (1996) and LIF measurements of Chu et al. (1999), are limited to maximum distances that fall within this transition region. Examples of existing spread data are shown in Fig. 2.

With this limitation on available experimental information, the 1/3 power law for the spread in the strongly advected region has not been confirmed. This power law is a direct result of the spread assumption. In addition, the constant in the spread relationship has not been confirmed for this region. Indeed, the value of the spread constant has been the subject of some debate. Traditionally, it has been assumed that the spread constant applicable in the weakly advected jet region is also applicable in the strongly advected region (Antonia and Bilger 1974; Knudsen 1988). However, Wright (1994) questions this assumption and, based on Chu's (1994) dominant eddy hypothesis, suggests the spread constant in the weak jet region should be half that in the strong jet region. After obtaining experimental data in a turbulent ambient environment in the weakly advected and transition regions of co-flowing jets, Chu et al. (1999) come to the same conclusion. However, without detailed experimental data from the strongly advected region, there is insufficient experimental evidence to support either approach.

There is a lack of experimental data in the strongly advected region because of the difficulties in making measurements in this region. In the strongly advected

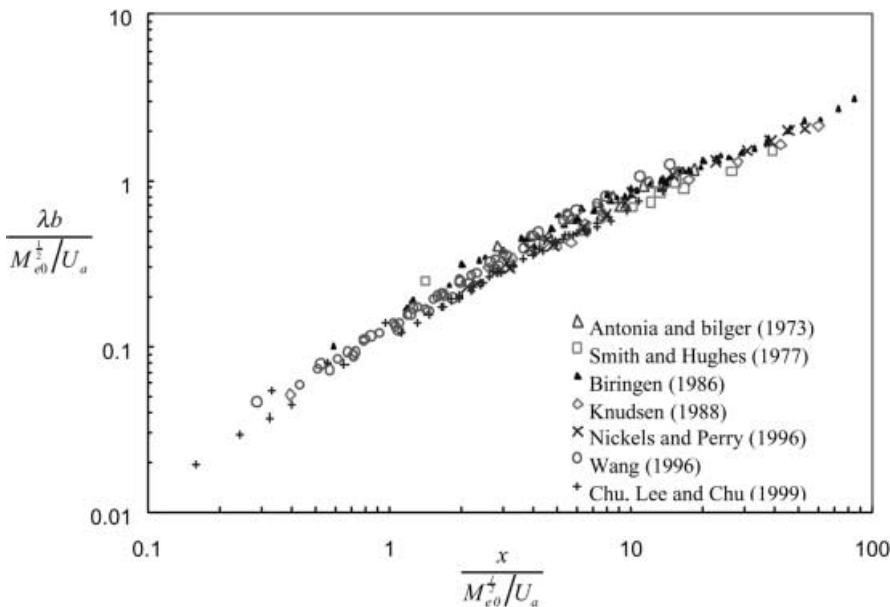


Fig. 2. Spread data obtained during previous investigations into the co-flowing jet problem. The value λ is assumed to be 1.19

region, the excess velocity signal is very small when compared with the ambient velocity. Hence an accurate determination of the difference between the absolute jet velocity and the ambient velocity is difficult. In addition, disturbances in the ambient fluid (such as ambient turbulence) have a significant influence on the flow behaviour in the strongly advected region. In Wang's (1996) experiments, the jet structure was completely destroyed by the presence of ambient turbulence, once the flow entered the transition region. This makes accurate measurements in a recirculating flume or wind tunnel difficult. Although minimizing the strength of the ambient turbulence can reduce its effects, the influences on the flow are still unknown. Conducting the experiments in a towing tank, where the ambient fluid remains stationary and the source is towed through it, further reduces the impact of the ambient turbulence. In this situation, the only turbulence generated is due to the discharge structure. The impact of this turbulence can be reduced by keeping the discharge structure small and by working with relatively low cross-flow Reynolds numbers. (This Reynolds number is based on the external pipe diameter and the ambient velocity.) The turbulence shed from the structure being therefore relatively weak. In addition, the discharge can be released so that a weakly advected jet forms near the source. In this way, the decaying ambient turbulence is largely entrained into the weakly advected flow, where it has little influence (Wang 1996), before the strongly advected jet forms.

While essentially eliminating the impact of turbulence, the latter approach presents a significant problem. Given that a weakly advected flow must form first and that the transition from weakly to strongly advected behaviour occurs over an order of magnitude of distance, measurements in the strongly advected region must be made at considerable distances from the source. In this context, tracer measurements are more feasible, because one can increase the strength of the source without altering the nature of flow.

2

Laser-induced fluorescence – a more traditional approach

When making concentration measurements the LIF technique has many advantages. These include its non-intrusive nature, the fact it provides information about the concentration field in a plane at an instant in time, and it also provides an excellent visualization of the flow. For the co-flowing jet experiment, it would be normal to set up an LIF system along the following lines. A laser light sheet would be positioned, along the flow centreline, at a fixed distance from the source and a tracer introduced into the source. In a towing tank, the light sheet and source would be towed at the same velocity, along the length of the tank, to simulate a co-flowing ambient current. While the source is towed, the intensity of the fluoresced light would be recorded and later analysed to yield concentration fields at regular time intervals. For higher ambient velocities, the experiments may be repeated several times to create a sufficient ensemble of data, so statistics that are representative of the flow behaviour can be obtained. Adjustments would be made to the distance between the source and the light sheet, so the flow behaviour can be observed at different distances from the source.

A set of experiments based on this approach was conducted in the Water Resources Laboratory at the Hong Kong University of Science and Technology, where the towing tank is 15 m in length, 2 m wide and 1.6 m deep. For these co-flowing jet experiments, the tank was filled with fresh water to a depth of 1.2 metres. The source consisted of a 1.77 mm (or a 4.64 mm) diameter pipe that was attached to a computer-controlled carriage, so that it discharged horizontally at a location 600 mm below the water surface. The initial discharge Reynolds number ranged from 2,100 to 2,650. The carriage was programmed to tow the source through the ambient fluid at a specified speed. The cross-flow Reynolds numbers for these experiments ranged from 16 to 750. Like the ambient fluid, the source fluid was fresh water and the densities of these fluids were accurately monitored using a precision density meter (PAAR DMA58). The tracer introduced into the source fluid was Rodamine 590. This dye fluoresces when illuminated with light of wavelength 514 nm and emits light at a wavelength of 590 nm. A Fluorometer (Sequoia-Turner 450) was used to monitor the initial tracer concentration for these experiments.

The 514 nm light source was generated using a 6 W argon laser operating in a single (green) mode with a power output of 2 W. The beam from the laser was carried to a beam scanning system via a fibre optic cable. The beam scanning system consisted of a rotating mirror, which scanned the laser beam across a parabolic mirror to create a parallel-planar light sheet. The light sheet generated was approximately 500 mm wide and 5 mm thick. The beam scanning system was mounted on a second carriage, which was towed by the carriage carrying the source. The distance between the two carriages was adjusted to observe the flow behaviour at different distances from the source.

The observation system was also mounted on the second carriage and it consisted of a low-light video camera (Panasonic WV-BP510/G). In all of the experiments, the Panasonic camera was operated such that its automatic light compensation features were inactivated. The camera was fitted with a filter that eliminated light at a wavelength of 514 nm, thus the only light recorded by the observation system was that generated by the fluorescing dye. The initial tracer concentration was adjusted so the jet was clearly visible to the video camera in the region of interest, while ensuring that the image was not saturated and light sheet attenuation was at acceptable levels. Information from the camera was recorded on a video recorder (Panasonic AG-6730) for subsequent digitization.

Ambient motions are of particular concern with this type of experiment, because the smallest motions can have a significant impact on the flow behaviour in the strongly advected region. A stilling mechanism, which consisted of a 100 mm × 2.0 m × 1.5 m fine filter mesh, was installed in the tank to assist in dissipating motions in the receiving water. Before the beginning of each experiment, the motion of particles in the tank was observed to ensure that the receiving water was still. A schematic diagram of the experimental system is shown in Fig. 3.

The video images were later digitized using a Data Translation (DT2867) image capture board and processed

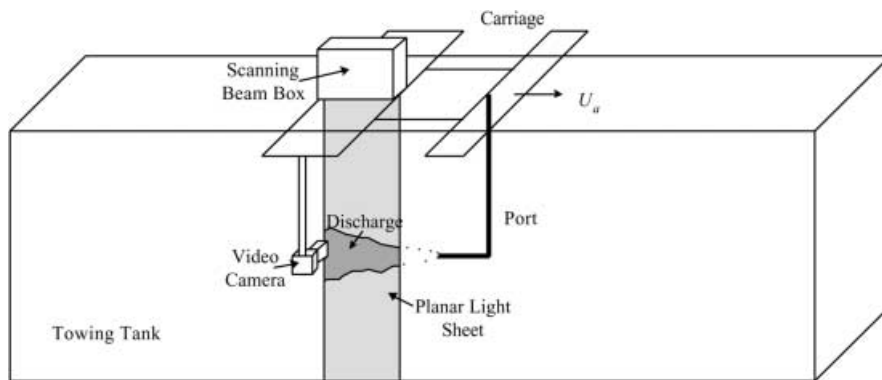


Fig. 3. A schematic diagram of the laboratory facility, that shows the towing tank and the LIF system

on a PC. The processing of the digitized images involved removing background light, correcting for variations in the sheet light intensity and calibrating the image. Upon the completion of these tasks, the intensity of light at each pixel was directly and consistently related to tracer concentration. Digitized images of a $50 \text{ mm} \times 50 \text{ mm}$ grid were also analysed to provide spatial calibrations for the images. This process revealed that each pixel in the images represents an area of approximately 0.5 mm^2 in the flow. Thus data were obtained from a measuring volume of approximately 3 mm^3 . This resolution is more than adequate for the present application, but concentration fluctuations on a scale smaller than this will be smoothed out. In addition, the images were normally sampled at 1 Hz, and this results in some temporal smoothing of the concentration fluctuation statistics. Typically, for each experiment in excess of two hundred images were captured. These images were averaged to provide details about the mean behaviour of the jets and in addition they were analysed to determine fluctuation statistics, such as the root-mean-square (rms) and the intermittency. Where appropriate, a tracer flux correction was applied to individual data sets and the details of this correction are given in Wang (2000). Spread data from the LIF system are shown in Fig. 4.

The data obtained with the present LIF system are more detailed than those obtained previously and we are able to reach dimensionless distances in excess of 100. However, measurements with the LIF system at these distances are difficult for two main reasons. First, the maximum distance over which the measurements are made is fixed ($\approx 500 \text{ mm}$). Therefore, relative to the distance from the source, the distance between the first and last data points of an individual experiment reduces as the distance from the source increases. For the experiments that were designed to obtain data at dimensionless distances in the region of 100, this relative distance had become so small that only a few meaningful data points could be obtained from each experiment.

Secondly, obtaining data at dimensionless distances of 100 requires an increase in the distance between the source carriage and the beam scanning system. This increase reduces the distance over which the source can be towed, because the tank is fixed in length, and hence the duration of an individual experiment. In addition, these experiments require relatively high ambient velocities, and this also reduces the duration of an individual experiment. Thus to obtain a sufficient ensemble of data for meaningful tracer statistics at a particular location, the number of repetitions of a particular experiment must increase.

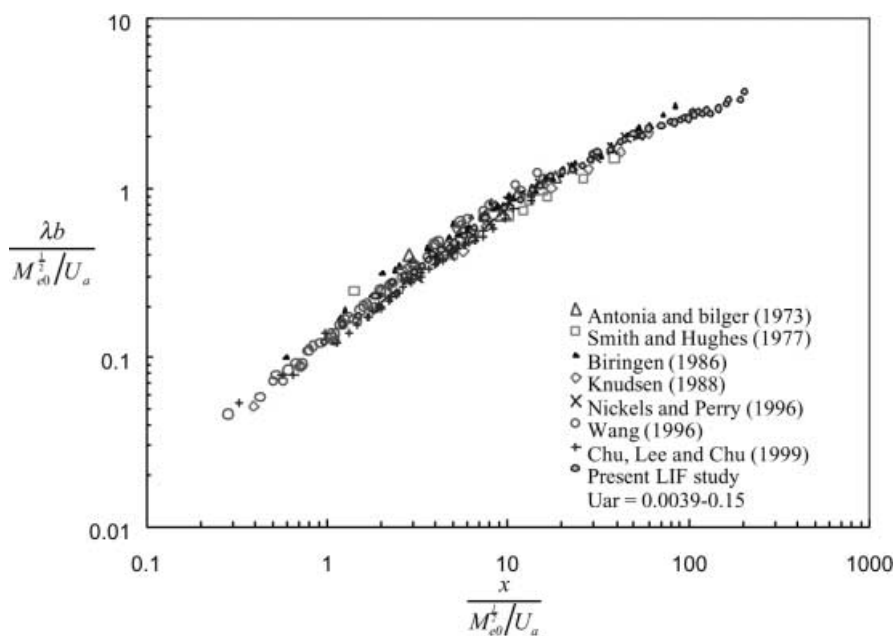


Fig. 4. Spread data obtained with the LIF system

The combination of reducing relative distances over which useful data can be obtained and the increasingly high number of repetitions for individual experiments, make measurements beyond dimensionless distances in the region of 100 impractical with the LIF system configured in this way. For these reasons, measurements were limited to the weakly advected and transition regions of the flow. In order to gather data in the strongly advected region of the flow in an effective and efficient manner, it is necessary to consider an alternative approach to the experimental and image processing systems outlined above.

3 The profile tracking system

One alternative is to fix the position of the light sheet and observation system, and to allow the source to move through and upstream of the sheet at a constant velocity. In relative terms, the light sheet then moves at a constant velocity away from the source. The difficulty with this approach is that the distance from the light sheet (and hence the images) to the source is constantly changing and, to obtain representative images at a given downstream location, the experiment would need to be repeated a very large number of times.

A digital time signal is superimposed on each video frame, so that the source's position relative to a marked location within an image can be determined. An initial reference time and location for the source can be determined, because the source passes through the region where the video camera is observing the flow behaviour (Fig. 6).

If a location is marked near the downstream edge of a particular image, as time progresses, the distance between this location (within subsequent images) and the source increases. However, if the marked location is allowed to move through the subsequent images at the ambient velocity, then the distance between the source and the marked location remains constant. Therefore the flow behaviour at this particular location can be observed for a period ($t_D = L_E/U_a$) during an individual experiment, where L_E is the distance over which the marked location is observed and this is less than or equal to the image length (L_I). A schematic diagram of the modified observation system is shown in Fig. 5. In Fig. 6 three instantaneous images taken from a profile tracking experiment are shown. The source can be seen moving through this sequence of images.

Given the minimum time (t_{\min}) required to obtain meaningful data at a particular location, the minimum number of experiments (N_E) required is then t_{\min}/t_D (rounded up to the nearest integer). Note the minimum time (t_{\min}) is normally in excess of 50 times the large eddy advection time scale $[b/(U_a + U_e/2)]$ for these experiments (Wang 2000). Concentration profiles at the marked location can therefore be tracked through a sequence of images and extracting information in this way greatly reduces the

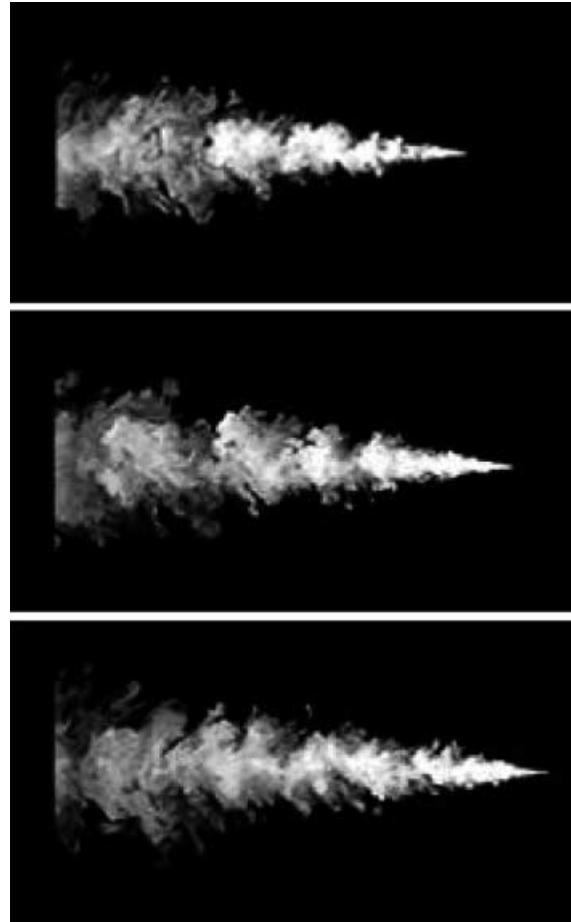


Fig. 6. Instantaneous images of a jet in co-flowing ambient fluid recorded in the initial stages of a PTS experiment. The observation system was stationary and the source was moving towards the right at 4 mm/s. The images were captured at 10-s intervals. The flow had an initial Reynolds number of 4,100 and an initial velocity ratio of 0.0018

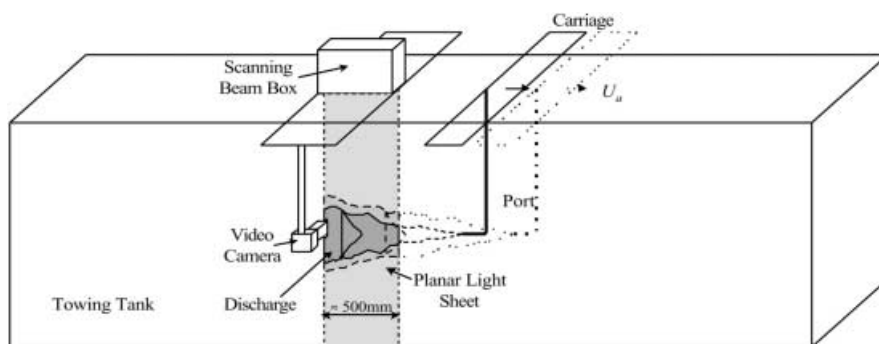


Fig. 5. A schematic diagram of the modified observation system, showing the source moving away from the light sheet and how a single concentration profile at a fixed distance from the source moves through the light sheet

number of repetitions required to obtain meaningful data. Such an approach largely overcomes the major problem associated with the alternative experimental configuration.

A significant advantage of the profile tracking method is that the length of the tank no longer limits the duration of an individual experiment. When the source reaches the end of the tank, it is in excess of 10 m from the observation area, and it can be shut off immediately. This allows the flow to continue to develop in the observation region, as the now imaginary source continues to move away from it. Alternatively, one can consider the source to be stationary and the camera system to be moving away from the source at the ambient velocity. The jet velocities in excess of the ambient velocity transport information concerning the change in source conditions. These excess velocities are relatively small, and hence it takes a considerable period of time for fluid in the region where the jet is shut off, to reach the observation area. This time varies for individual experiments, but it allows measurements to continue after the source has reached the end of the towing tank. Hence the distances from the source at which observations can be made are considerably larger than those made with a normal LIF system.

The flexible duration of the experiments also makes it possible to work with higher ambient velocities. This is a considerable advantage, because the scale of the flow is reduced, making measurements at greater distances possible. In addition, higher ambient velocities result in the strongly advected flow region developing in relatively close proximity to the source.

Central to the method is the ability to track concentration profiles at a given location through a sequence of images. This requires that modifications be made to the image processing system. Indeed, images are no longer dealt with as a whole, but instead profiles at specified locations in the images are extracted for processing and further analysis. The profiles are processed in much the same way as for the LIF experiments, so that the profile intensities are consistently related to tracer concentration. The extraction of these profiles begins near the downstream edge of a particular image. The location in the image where the extraction begins is user specified, as is the upstream location where the profile extraction terminates in a subsequent image. In between profiles are extracted from a sequence of images at regular intervals defined by $U_a \Delta t$, where Δt is the time step for profile extraction. This is done so that the distance from the source at which data are gathered remains unchanged. The number of profiles per downstream location per experiment (N_p) is then $L_E / (U_a \Delta t)$. The image location at which the profile extraction terminates is adjusted, so that N_p is an integer.

The location of each subsequent profile within an image is calculated with reference to the location of the initial profile and then converted to an integer pixel location using appropriate scaling factors. This approach avoids the accumulation of round-off errors, but there is some spatial dithering of the intensities (of the order of 1 pixel) because of the round-off error introduced when the real distance is scaled to an integer pixel value. Where the distances from the source are small, this error can be

eliminated through careful selection of the ambient velocity and the profile extraction rate. In addition, any mismatch between the camera-framing rate (25 frames per second) and the profile extraction rate introduces an error in locating the profile (Wang 2000). However, for the experiments presented here, this error was small, being less than 1% in the worst case.

Once the extraction of profiles at a particular distance from the source is complete, the extraction procedure can begin at a different downstream location. It is possible to introduce a time delay at this point to increase the distance between samples. The considerable flexibility in defining the distance between the downstream locations where data are collected is another important advantage of PTS. The ability to increase the distance between observation points beyond the image length, as the distance from the source becomes large, allows data to be collected over an appropriately large distance for these experiments. This is particularly useful when the tracer concentration decays slowly with distance. Alternatively, if it is desirable to collect data where the distance between observation points is relatively small (close to the source), information from multiple locations can be extracted from each sequence of images. Thus an appropriate range for recording the data can be determined for each experimental configuration, whether the data are being recorded close to or far from the source.

It is also possible to set an initial time delay, so that extraction does not begin until the source has moved a specified distance away from the observation area. Where an ensemble of data from different experiments is to be analysed, it is essential that the starting point for the extractions from the different experiments be the same (as well as all the other parameters pertaining to the PTS). This can be achieved by starting the extraction when the source is in the same on screen location for each of the experiments.

Typical values of PTS and other experimental parameters for the co-flowing jet experiments conducted with the PTS system are listed in Table 1. In this example, it is worth noting that the use of profile tracking enables 41 profiles to be obtained at each location, relative to the source, for an individual experiment. Without profile tracking, a single profile would be obtained at each location and many more experiments would be needed to obtain meaningful statistics from the data.

The PTS system is an extension of the original LIF system developed for the Water Resources Laboratory at the Hong Kong University of Science and Technology (Davidson and Pun 1999), and hence the software that drives it has been written in the same language (ASYST).

4 LIF and PTS compared

In comparing measurements made by the LIF and PTS systems, we begin with mean concentration profiles, where c is the local mean concentration. Data from both systems are presented in Fig. 7. The agreement between LIF and PTS data is very good, providing confidence in the PTS's ability to measure mean quantities relative to the mean centreline concentration and the flow spread. The con-

Table 1. Experimental parameters for the PTS co-flowing jet experiments

Experimental parameter	Sample values	Description and comments
Horizontal scaling factor H_{SCL} (mm/pixel)	0.72	Determined from the spatial calibration of the image. This can be adjusted locally if image distortion becomes significant.
Ambient velocity U_a (mm/s)	60	Determined from experimental design.
Profile sampling rate Δt (ms)	168	Adjusted so as to make the value of $U_a\Delta t/H_{SCL}$ an integer.
Distance between profiles (mm)	10.1	$U_a\Delta t$
Initial image offset O_I (pixel)	90	Needed to eliminate image regions that have not been calibrated.
Final image offset O_F (pixel)	118	Needed to eliminate the image regions that have not been calibrated.
Image length L_I (mm)	553.0	Images are 768 pixels in length and hence the image length, in its simplest form, is given by $768 H_{SCL}$.
Effective image length L_E (mm)	403.2	Length of image from which profiles will be extracted and this is given by $(768 - O_I - O_F)H_{SCL}$.
Profiles per image length N_p	41	$L_E/(U_a\Delta t) + 1$
Sampling time per source location t_D (s)	6.72	$(N_p - 1)\Delta t$
Distance between sample locations (mm)	413.3	$N_p U_a\Delta t$
No. of sample locations	20	Determined from the total image recording time and the sampling time per source location

centration profiles are clearly Gaussian and self-similar in the weakly advected and transition regions where the LIF system and PTS are compared.

The Gaussian profiles shown in Fig. 7 are scaled based on the mean centreline concentration and spread data, which have been obtained from each profile through a least-squares fit of the Gaussian distribution. In Figs. 8 and 9, the spread and centreline dilution data obtained with the PTS and LIF systems are shown. The dilution and spread data obtained with the LIF and PTS systems show very good agreement in the weakly advected and transition

regions. The PTS system can therefore be employed to measure data in the strongly advected region with confidence. Indeed, data obtained with the PTS system extend well beyond those obtained with the LIF system and well into the strongly advected region. Both data sets provide information about the co-flowing jet behaviour at non-dimensional distances in excess of data obtained from previous investigations and, in the case of PTS, the difference is an order of magnitude.

The main purpose of presenting the data in the strongly advected region is to demonstrate how the PTS can be effectively employed to make measurements at previously inaccessible distances from the flow source. We will not therefore enter into a detailed discussion of the implications of these data. However, the data do confirm the power laws for dilution and spread in the strongly advected region, but the implications for model closure are more complex and are discussed in detail in Davidson and Wang (in preparation), where additional data sets obtained with the PTS are also presented.

A major limitation of the LIF system becomes apparent in the transition regions shown in Figs. 8 and 9, where with each experiment the LIF system provides information over an increasingly smaller relative distance. Many experiments are therefore required to build up a picture of mean flow behaviour over the distances considered here. In contrast, a single set of PTS experiments provide information on the flow behaviour over a wide range (an order of magnitude) of dimensionless distance, giving a complete picture of the mean flow behaviour with a relatively small number of experiments.

It is equally important that the PTS provide accurate information about the nature of the concentration fluctu-

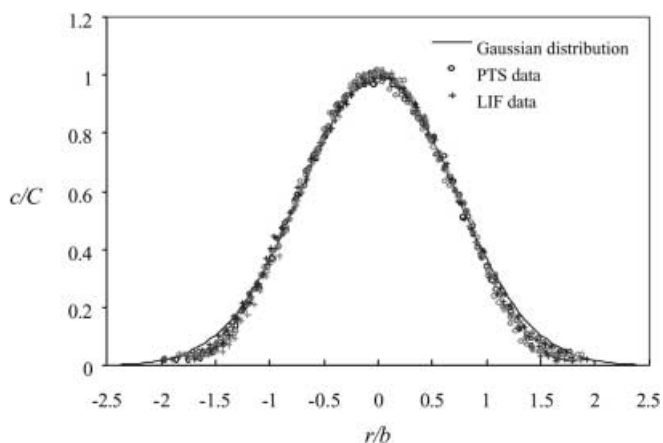


Fig. 7. A comparison of mean concentration profiles from the LIF and PTS systems. The data presented are taken from experiments with initial velocity ratios ranging from 0.00385 to 0.01412 and at dimensionless downstream locations varying from 0.86 to 3.54

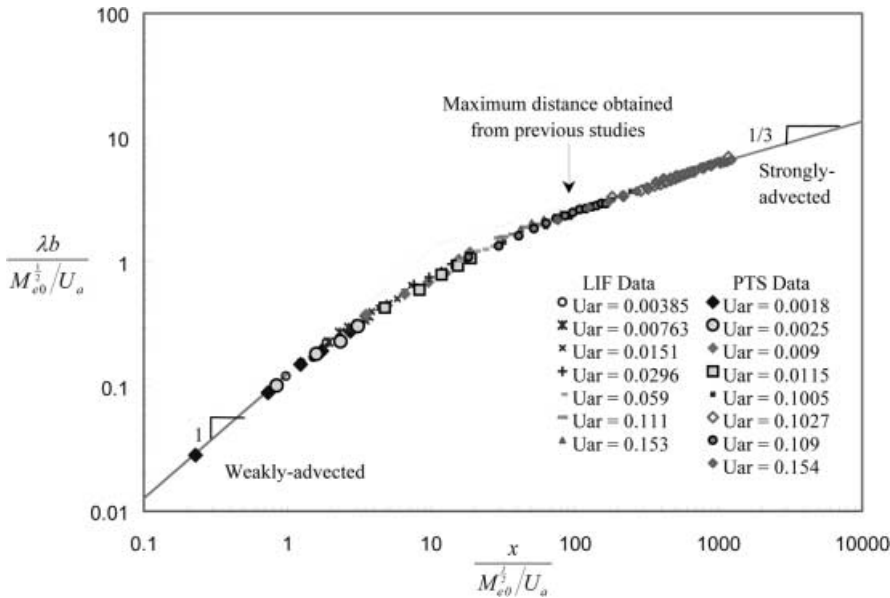


Fig. 8. Spread data from the PTS and LIF systems for the co-flowing jet problem

tuations within the flow. A common way to represent this information is through calculation of the rms of the concentration signal and the probability of exceeding a specified minimum value of concentration (intermittency). This specified minimum value was set just above the background concentration level for the current analysis. In Figs. 10 and 11, the fluctuation statistics are compared using data from the weakly advected and transition regions (where the LIF system operated effectively). The agreement between the PTS and LIF systems is generally very good, indicating that the PTS provides accurate information about the concentration fluctuations as well as the mean quantities. It is worth noting that comparisons of fluctuation statistics have been limited to maximum dimensionless distances of approximately 4. This is because the magnitudes of these statistics become dependent on downstream distance further into the

transition zone, making comparisons considerably more difficult.

5 Conclusions

The problem of obtaining high-quality data at considerable distances from the flow source has been addressed through the development of a PTS. The value of this system has been demonstrated for the co-flowing jet problem, where it is necessary to gather data at large distances from the flow source. The experiments were conducted in a towing tank, and the laser sheet and observation system remained stationary while the source moved downstream. The image processing system was then used to track concentration profiles at a particular downstream location through a sequence of images. In this way, multiple profiles were collected at each downstream location for an

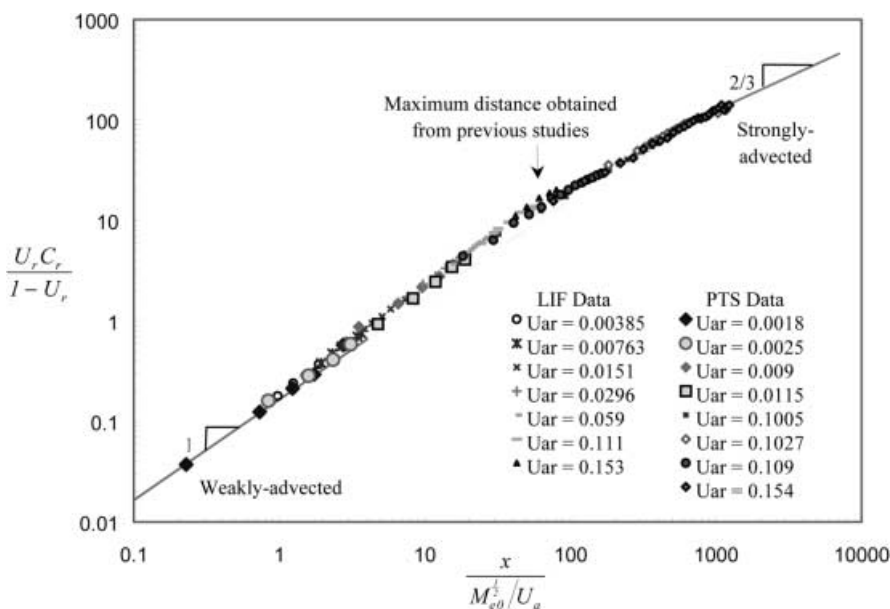


Fig. 9. Mean centreline dilution data from the PTS and LIF systems for the co-flowing jet problem

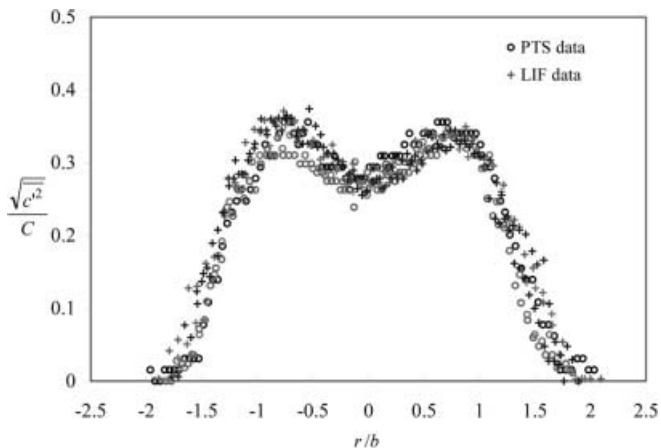


Fig. 10. Root-mean-square data from the PTS and LIF systems for the co-flowing jet problem. The data presented were taken from experiments with initial velocity ratios ranging from 0.00385 to 0.01412 and for dimensionless distances ranging from 1.55 to 3.71

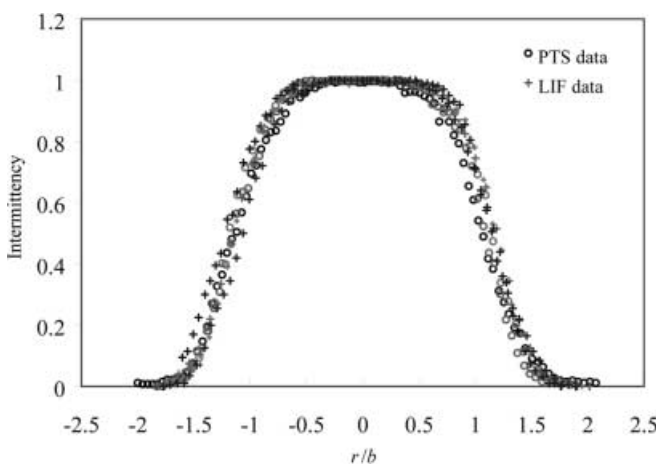


Fig. 11. Intermittency data from the PTS and LIF systems for the co-flowing jet problem. The data presented were taken from experiments with initial velocity ratios ranging from 0.00385 to 0.01412 and for dimensionless distances ranging from 1.55 to 3.71

experiment. The profile tracking system significantly reduced the number of repetitions required to obtain reliable data for a given discharge configuration, making it possible to obtain data at large distances from the flow source. Comparisons with data obtained from an LIF system show that the PTS is able to accurately measure the mean and fluctuating behaviour of a co-flowing jet, and the PTS has been employed to gather data at previously inaccessible distances from the jet source.

The PTS has significant advantages over a normally configured LIF system. With PTS there is more flexibility in terms of the duration of the experiment, because the source can be shut off when it reaches the end of the towing tank without immediately affecting the flow in the observation area. This enhances the system's ability to make observations at much greater distances from the flow source, when compared with LIF. In addition, there

is considerable flexibility in defining the spacing between the downstream locations where data are gathered. Close to the source, data can be collected such that the spacing is less than the image length and, at large distances from the source, the spacing can be increased beyond the image length. The PTS therefore allows data to be gathered over an appropriate distance range, where this range is dependent on the distance from the source at which the data are being collected and also how rapidly the data are varying. Finally, the extended duration of the PTS enables experiments to be conducted at relatively high ambient velocities, again improving our ability to record detailed information at relatively large distances from the source.

References

- Antonia TA; Bilger RW (1973)** An experimental investigation of an axisymmetric jet in a coflowing air stream. *J Fluid Mech* 61: 805–822
- Antonia TA; Bilger RW (1974)** The prediction of the axisymmetric turbulent jet issuing into a co-flowing stream. *Aeronaut Q* 251: 69–80
- Biringer S (1986)** An experimental investigation of a turbulent round jet in a coflowing airstream. Paper presented at the ASME winter annual meeting, Anaheim, Calif.
- Chu PCK; Lee JH; Chu VH (1999)** Spreading of turbulent round jet in a coflow. *J Hydraul Eng ASCE* 125: 193–204
- Chu VH (1994)** Lagrangian scaling of turbulent jets and plumes with dominant eddies. In: Davies PA, Valente Neves MJ (eds) *Recent research advances in the fluid mechanics of turbulent jets and plumes*. Kluwer Academic, Dordrecht, pp 45–72
- Davidson MJ; Pun KL (1998)** Hybrid model for the prediction of initial dilutions from outfall discharges. *J Hydraul Eng ASCE* 124: 1188–1197
- Davidson MJ; Pun KL (1999)** Weakly advected jets in cross-flow. *J Hydraul Eng ASCE* 125: 47–58
- Davidson MJ; Wang HJ (in preparation)** A strongly-advected jet in a coflow. *J Hydraul Eng ASCE*
- Knudsen M (1988)** Buoyant horizontal jets in an ambient flow. PhD Thesis, Rep. 88-7, Department of Civil Engineering, University of Canterbury, Christchurch, New Zealand
- Nickels TB; Perry AE (1996)** An experimental and theoretical study of the turbulent coflowing jet. *J Fluid Mech* 309: 157–182
- Papantoniou D; List EJ (1989)** Large-scale structure in the far field of buoyant jets. *J Fluid Mech* 209: 151–190
- Patel RP (1971)** Turbulent jets and wall jets in uniform streaming flow. *Aeronaut Q XXII*: 311–326
- Pun KL (1999)** Hybrid models for jets and plumes in a flowing ambient fluid. PhD Thesis, Department of Civil Engineering, The Hong Kong University of Science and Technology, Hong Kong
- Smith DJ; Hughes T (1977)** Some measurements in a turbulent circular jet in the presence of a co-flowing free stream. *Aeronaut Q XXVIII*: 185–196
- Wang HJ (1996)** An experimental study of single and multiple jets in a coflowing environment. MPhil Thesis, Department of Civil and Structural Engineering, The Hong Kong University of Science and Technology, Hong Kong
- Wang HJ (2000)** Jet interaction in still and moving environments. PhD Thesis, Department of Civil and Structural Engineering, The Hong Kong University of Science and Technology, Hong Kong
- Wright SJ (1994)** The effect of ambient turbulence on jet mixing. In: Davies PA, Valente Neves MJ (eds) *Recent research advances in the fluid mechanics of turbulent jets and plumes*. Kluwer Academic, Dordrecht, pp 13–27